JACS
JOURNAL OF THE AMERICAN CHEMICAL SOCIETY
Communication
pubs.acs.org/JACS

Growth of Horizontal Semiconducting SWNT Arrays with Density Higher than 100 tubes/μm using Ethanol/Methane Chemical Vapor Deposition

Lixing Kang,[†,‡,§] Shuchen Zhang,[†] Qingwen Li,[‡] and Jin Zhang*[,†]

[†]Center for Nanochemistry, Beijing Science and Engineering Center for Nanocarbons, Beijing National Laboratory for Molecular Sciences, College of Chemistry and Molecular Engineering, Peking University, Beijing 100871, P. R. China

[‡]Division of Advanced Nanomaterials, Suzhou Institute of Nanotech and Nanobionics, Chinese Academy of Sciences, Suzhou 215123, P. R. China

[§]University of Chinese Academy of Sciences, Beijing 100049, P. R. China

Supporting Information

ABSTRACT: Horizontally aligned semiconducting single-walled carbon nanotube (s-SWNT) arrays with a certain density are highly desirable for future electronic devices. However, obtaining s-SWNT arrays with simultaneously high purity and high density is extremely challenging. We report herein a rational approach, using ethanol/methane chemical vapor deposition, to grow SWNT arrays with a s-SWNT ratio over 91% and a density higher than 100 tubes/μm. In this approach, at a certain temperature, ethanol was fully thermally decomposed to feed carbon atoms for Trojan-Mo catalysts growing high density SWNT arrays, while the incomplete pyrolysis of methane provided appropriate active H radicals with the help of catalytic sapphire surface to inhibit metallic SWNT (m-SWNT) growth. The synergistic effect of ethanol/methane mixtures resulted in enriched semiconducting SWNTs and no obvious decrease in nanotube density due to their milder reactivity and higher controllability at suitable growth conditions. This work represents a step forward in large-area synthesis of high density s-SWNT arrays on substrates and demonstrates potential applications in scalable carbon nanotube electronics.

Nowadays, silicon transistors are approaching a bottleneck with devices becoming smaller.[1] Horizontally aligned single-walled carbon nanotubes (SWNTs) have been considered as one of the most viable candidates for future transistor technologies due to their exceptional device performance.[2] For SWNT-based transistor applications to be realized, the density of SWNT arrays would need to be more than 125 tubes/μm and the impurity concentration of metallic SWNTs (m-SWNTs) less than 0.0001%.[3] Currently, direct growth of high-quality and aligned SWNTs on substrates by chemical vapor deposition (CVD) is a promising strategy to meet the requirement of high-performance devices.

Over the past few decades, notable progress has been made in controllable synthesis of SWNT arrays using the CVD method.[4,5] As for the density, through sequentially patterning catalysts,[6] multiple-cycle growth,[7] and periodic growth,[8] 10−60 tubes/μm aligned SWNTs have been obtained on quartz substrates. Recently, our group developed newly designed catalysts called Trojan (Fe)[9] and Trojan-Mo (Fe/Mo),[10] which realized over 130 tubes/μm on sapphire surface. However, these approaches show no semiconducting (s-) selectivity. For increasing the s-SWNT percent during growth, the most widely used technique was to introduce etching species, including water,[11] methanol,[12] isopropyl alcohol,[13] and hydrogen,[14] to remove m-SWNTs. Accordingly, 84−97% semiconducting nanotubes were obtained in the arrays. However, these strategies severely decreased the densities of the obtained s-SWNT arrays, and general results did not exceed 10 tubes/μm. On the basis of the Trojan-Mo catalyst, we also made an effort to use the usual etchants mentioned above to obtain high density s-SWNTs; however, the high density and selectivity could not coexist. When using water or methanol as etchants, the selectivity was high, but the density decreased significantly. As for using isopropyl alcohol as the carbon feedstock, the density had no obvious change but also no selectivity. Varying the hydrogen flow, there was a decline in the density but no change in the selectivity. These attempts indicated the very narrow growth window and parameter space of these usual etchants. Thus, how to choose a more suitable etchant in our Trojan-Mo system is a key issue for balancing density and selectivity.

In the CVD system, the carbon precursor is an important factor affecting the properties of the produced SWNT arrays. Methane, as one of the most commonly used precursors for growing SWNTs, is more stable than other carbon sources like ethanol, ethylene, and acetylene due to its stronger C−H bond.[15] The pyrolysis of methane for synthesis of SWNTs usually requires above 900 °C to become thermodynamically allowed.[16,17] When the temperature decreases to around 800 °C (the normal SWNT growth condition using ethanol), methane fails to supply carbon species with SWNT formation, whereas in the presence of metal catalysts or catalyzing substrate material, methane adsorbs and dissociates on their surface. Then, some carbon depositions, H radicals, and other hydrocarbons are produced from the incomplete decomposition of methane.[18] The activated H radicals from methane plasma or hyperthermal hydrogen (e.g., > 1000 °C) have been confirmed to selectively

Received: April 6, 2016
Published: May 13, 2016

DOI: 10.1021/jacs.6b03527
J. Am. Chem. Soc. 2016, 138, 6727−6730

react with metallic nanotubes through hydrogenation reaction.[19,20] However, the methane plasma or hyperthermal hydrogen are highly reactive and hard to control, which are always accompanied by a diminished yield of s-SWNTs. By contrast, the dissociated H radicals from the catalytic cracking of methane under certain temperatures are much milder and more controllable. Therefore, it seems possible to increase s-SWNT percent and maintain high density in the SWNT arrays by introducing appropriate amounts of methane during the CVD process.

In this study, we provide a reliable method that combines "Trojan-Mo catalysts" with ethanol/methane CVD, simultaneously achieving high density and high semiconducting selectivity of SWNT arrays over large areas. Figure 1a schematically illustrates the procedure for this method. Under certain temperatures, ethanol was fully thermally decomposed to feed carbon atoms for Trojan-Mo catalysts growing high density SWNT arrays, whereas methane was catalytically cracked to provide appropriate active H radicals on the substrate to inhibit m-SWNT growth. Ethanol and methane cooperated to achieve both high density and high selectivity in SWNT arrays.

Scanning electron microscopy (SEM) and high-resolution transmission electron microscopy (HRTEM) images presented in Figure 1b–d show typical results using an ethanol/methane mixture (50 sccm Ar through an ethanol bubbler and 100 sccm methane) as carbon source. The entire sapphire substrate was uniformly covered with high density SWNT arrays (see Figure S1). More than 100 tubes per micrometer in certain regions were as shown in the high multiplying SEM image (inset in Figure 1c) and TEM image (inset in Figure 1d). However, at present, it still meets a big challenge to obtain a larger area (wafer scale) with well-distributed density as high as 100 tubes/μm and submicrometer uniformity using ethanol/methane CVD. The atomic force microscopy (AFM) image (Figure 1e) showed a dense array of parallel SWNTs with the main diameter distribution from 0.8 to 1.6 nm (Figure S2).

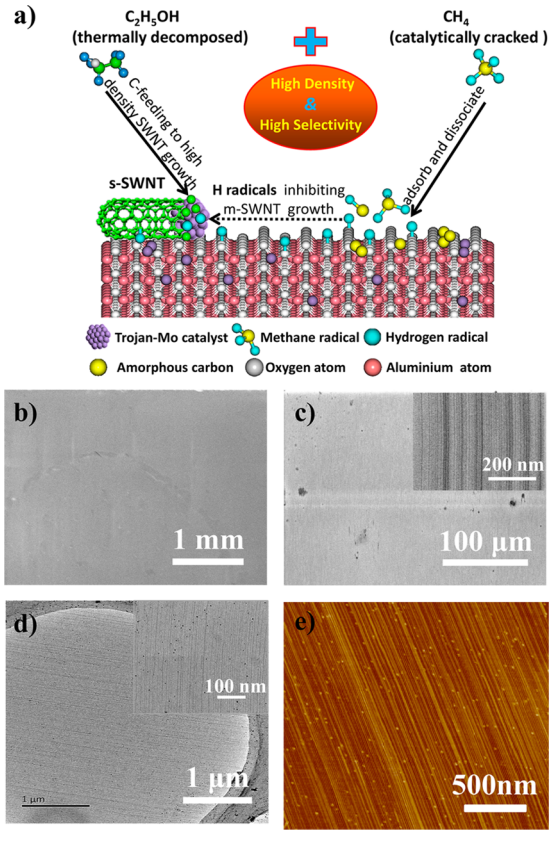

Figure 1. (a) Schematic illustration of selective growth of high density s-SWNTs by ethanol/methane CVD. (b,c) SEM images of the as-grown SWNT arrays. (d) HRTEM images of the SWNT arrays transferred onto the ultrathin carbon membrane supported on a copper grid. (e) Typical AFM image of the SWNT arrays.

To characterize electronic properties of the as-grown SWNT arrays, we combined three methods including multiple excitation lasers for Raman, ultraviolet/visible/near-infrared (UV–vis–NIR) absorption spectrum, and electrical measurements. Raman line mapping with different lasers at the same place was executed to calculate the abundance of semiconducting tubes in the SWNT array. In Figure 2a, typical radial breathing mode (RBM) of the Raman spectra with a 488 nm excitation laser showed that s-SWNT peaks were the overwhelming majority. The statistics of the RBM in the Raman measurements of multi-batch samples (Figure 2b) gave an estimate of 94.6% based on the detected tubes. Representative test results using other excitation lasers (wavelengths of 514, 633, and 785 nm) are shown in Figure S3a–c. In addition, the corresponding tangential vibration (G mode) bands at ~1580 cm^{-1} did not exhibit the Breit–Wigner–Fano (BWF) line shapes (see Figure S3d), a typical feature of metallic SWNTs, further confirming the semiconducting characteristic of the nanotubes.[21] Meanwhile, nonsharp D bands indicated that the synthesized s-SWNTs were of high quality (Figure S3d).

Because of the limitation of Raman measurements, only parts of SWNTs in the arrays resonate with the discrete excitation

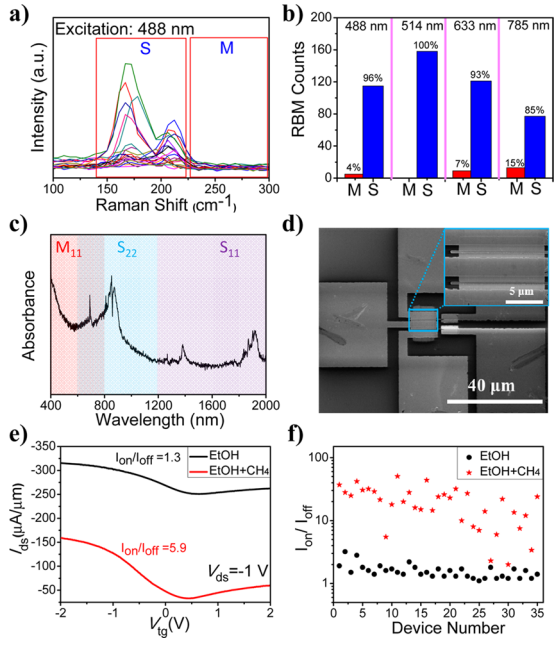

Figure 2. (a) RBM peaks of the Raman spectra for the as-grown SWNT samples with 488 nm excitation. (b) Multiwavelength laser Raman statistics of m- and s-SWNTs in the samples. (c) UV–vis–NIR spectrum after background subtraction. (d) SEM images of top-gate FET devices fabricated on a sapphire substrate. (e) Comparison of the transfer characteristic curves of the as-grown SWNT device with and without methane. (f) Statistical result of I_{on}/I_{off} ratios for each device.

DOI: 10.1021/jacs.6b03527
J. Am. Chem. Soc. 2016, 138, 6727–6730

wavelengths.[21] UV−vis−NIR absorption spectrograph was a powerful tool to evaluate the abundance of s-SWNTs.[22] However, the low duty ratio of horizontally aligned SWNT arrays on the sapphire surface (maximum value of <10%) largely decreases the detected signal intensity. Thus, we multiple-transferred the high density s-SWNT samples onto the transparent fused quartz for UV−vis−NIR measurements. More details are given in the Experimental Section of the Supporting Information. The morphology of the multiple-transferred SWNT array was shown in an AFM image in Figure S4a. According to the UV−vis−NIR spectrum after background subtraction (Figure 2c and Figure S4b), the content of s-SWNTs was approximately 93% (for calculation details, see the description in Figure S4b).

For the s-SWNT enrichment in the nanotube arrays to be further verified, top-gate field-effect transistors (FETs) were directly fabricated from the as-grown SWNTs on sapphire for electrical measurements (for details, see the Experimental Section). Figure 2d shows the SEM image of a typical FET device with a gate length of 0.5 μm and a channel width of 15 μm. Figure 2e presents the transfer characteristic curves of devices based on the as-grown SWNTs with and without methane. The introduction of methane obviously enhanced the on/off ratio. A number of similar FET devices with different channel length from multi-batch samples were measured, and the on/off ratio distribution was plotted in Figure 2f. In the case of using ethanol only, three SWNT devices had an on/off ratio larger than 2 out of 35 devices. As for nanotubes from ethanol and methane-mixed CVD, the best on/off ratio was 50.6, and the median value was 21.5. Overall, 91.4% of SWNT devices (32 out of 35) exhibited an on/off ratio higher than 5.

More $I-V$ curves of the FETs are shown in Figure S5. On the basis of the mean conductance of m-SWNTs to s-SWNTs being 2.5 in our samples, the on/off ratio value of 5 corresponded to the contents of the semiconducting tubes up to 91% (for details of the calculation, see the description in Figure S5). Thus, the estimated contents of s-SWNTs in mixed carbon source CVD was approximately 91% by electrical measurements, consistent with the results obtained by Raman and UV−vis−NIR absorption measurements.

To explore the role of methane in the selective growth of s-SWNTs, we set 50 sccm of argon through an ethanol bubbler and varied the flow rate of methane. Figure 3a shows typical RBM peaks of the SWNTs obtained by adding different methane fluxes with 633 nm excitation. There was an optimum methane flow (100 sccm) for obtaining a high percentage of s-SWNTs. As for the density, it decreased with the increase of methane flux (Figure 3b). In comparison to pure ethanol CVD, AFM images (Figure 3c and Figure S6) showed that the sapphire substrates became dirty and had many nanoparticles on surface after ethanol/methane growth. These nanoparticles were mainly carbon deposited or carbon deposit-coated Trojan-Mo catalysts, which was confirmed below. As shown in Figure 3d, when a relatively low methane flow (30 or 100 sccm) was introduced, the average diameters of the carbons deposited were around 3 nm. These minor adsorbed carbons just slightly lowered the density but significantly improved the s-SWNT selectivity (Figure 3b). However, the sizes of the carbons deposited were significantly larger when the methane flow exceeded 100 sccm. The heavy carbons that were deposited distinctly influenced the yield and alignment of SWNT arrays (Figure S6c). Meanwhile, the selectivity dropped significantly. When only methane was used as the carbon source, no SWNTs

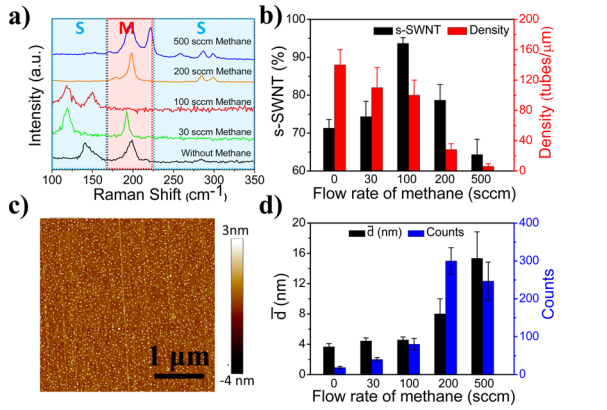

Figure 3. (a) Typical RBM peaks of the SWNTs obtained by adding different methane flows with 633 nm excitation. (b) Statistics of density and s-SWNT percent with different methane flows. (c) AFM image of the SWNT sample obtained by adding 200 sccm methane. (d) Statistics of counts and average diameters of carbon deposits with different methane flows in a given area (3 μm × 3 μm) on a sapphire substrate.

were found (Figure S7a), but dense nanoparticles were on the substrate (Figure S7b), which proved the existence of disordered carbon with turbostratic structure by Raman measurements (Figure S7c). Though methane could not produce nanotubes at our growth temperature (830 °C), they generated carbon depositions and H radicals on the substrate. The activated H radicals tended to saturate the dangling bonds of metallic nanotubes and, in situ, inhibited their growth due to their lower ionization energy.[23] Because the H radicals from the dissociation of methane were more moderate and suitable compared with those of other etchants containing oxygen or high energy radicals, high density s-SWNT arrays were thus successfully obtained.

Because of this dual role of the hydrogen radical,[16] it was very important to control the amount and reactivity. When the growth temperature increased, the density of the arrays dropped markedly to less than 5 tubes/μm at 950 °C (Figure 4a). The alignment of the SWNTs also became worse (Figure 4b). Meanwhile, a significant number of metallic peaks were found in these samples (Figure 4c). Similar growth results at 870 °C and 910 °C are shown in Figure S8. At higher temperature, the methane cracked into more hydrogen radicals with higher activity and stronger etching ability, resulting in the loss of selective growth. For the etching property of hydrogen radicals

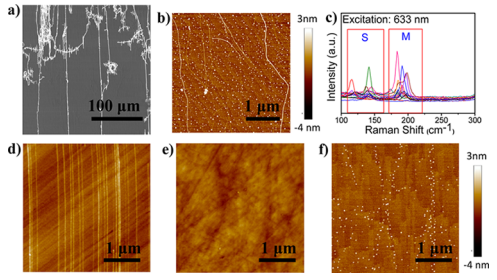

Figure 4. SEM (a) and AFM (b) images of the SWNT arrays grown from ethanol/methane at 950 °C. (c) RBM peaks of the SWNT arrays with 633 nm excitation. (d) Typical AFM image of the as-grown SWNT arrays on quartz. (e,f) AFM images of blank quartz and sapphire substrates, respectively, under the same growth conditions (with only methane as the carbon source). The Z-scales in the AFM images (d−f) were the same.

DOI: 10.1021/jacs.6b03527
J. Am. Chem. Soc. 2016, 138, 6727−6730

from methane to be further investigated, the SWNT arrays after normal ethanol growth were kept at the same temperature and 100 sccm of methane was introduced for 15 min. The density of the arrays decreased to 15 tubes/μm. Some of the SWNTs had been destroyed into fractions (Figure S9a). Raman characterization showed obvious metallic tube signals (Figure S9b). These results indicated that hydrogen radicals from methane did have the ability to attack and destroy the SWNTs under the CVD conditions. However, the selectivity of growing s-SWNTs could only happen during the initial stage of SWNT growth. At that point, the chemical reactivity difference between metallic and semiconducting nanotubes was the most obvious.

Another essential factor for the selective growth is the sapphire substrate. Using a single metal catalyst (Trojan or Mo), we still obtained semiconducting-enriched SWNT arrays on the sapphire surface through optimizing the flow rate of methane/ethanol (Figure S10a). For the Mo catalyst in particular, a similar selectivity of s-SWNTs (~90%) was obtained under suitable methane/ethanol flows, whereas the density decreased to below 10 tubes/μm (Figure S10b). However, this trend was not observed on the ST-cut single crystal quartz substrate. We varied the Mo/Fe ratio and the methane flow, yet no noticeable change in the percent of s-SWNTs was observed (Figure S10c). Furthermore, upon changing the catalyst deposition method on sapphire to be the same as on quartz, similar s-SWNT selectivity still existed (Figure S10d). An AFM image (Figure 4d) showed only a small amount of carbon deposition on the quartz surface after SWNT growth. Moreover, comparing the surface morphology of blank quartz and sapphire substrate after the same pure methane growth (Figure 4e,f), the amount of carbon deposition on sapphire was far more than that on quartz. In vertical SWNT array growth, Al_2O_3 has been the most widely adopted because of its ability to promote hydrocarbon reforming.[24] Thus, we concluded that methane was easier to adsorb and dissociate on sapphire than quartz, which could result in the difference in the semiconducting selectivity. Nevertheless, because of the complicated interplay of many factors in SWNT growth, there might be other underlying factors affecting the selective growth process. Further exploration is currently underway.

In conclusion, we have developed an effective method to grow large area, high-density, semiconducting-enriched SWNT arrays using ethanol/methane CVD. The density of the arrays was as high as 100 tubes/μm. Raman spectra, UV−vis−NIR absorption spectra, and electrical measurements demonstrated over 91% semiconducting tubes in the SWNT arrays. Through a systematic investigation of the effect of methane on the SWNT growth, we propose that the selectivity originates from methane adsorbed and dissociated on the sapphire surface to generate H radicals. These moderate and appropriate H radicals create a suitable etching environment for in situ inhibition of m-SWNT growth. Meanwhile, the density of the arrays had no obvious decrease due to milder reactivity and higher controllability of the H radicals from incompletely decomposed methane. The ethanol/methane CVD method successfully overcame the discrepancy between the high density and semiconducting selectivity of SWNT arrays. In other words, this work provides a possible choice for the growth of aligned high density and semiconducting SWNTs and shows potential for application in future carbon nanotube-based nanoelectronics.

■ ASSOCIATED CONTENT

Supporting Information

The Supporting Information is available free of charge on the ACS Publications website at DOI: 10.1021/jacs.6b03527.

Experimental details, characterization methods, and supplementary figures, including SEM and AFM images RBM peaks from Raman spectra, $I-V$ curves, and statistical analyses (PDF)

■ AUTHOR INFORMATION

Corresponding Author

*jinzhang@pku.edu.cn

Notes

The authors declare no competing financial interest.

■ ACKNOWLEDGMENTS

This work was supported by the NSFC (21233001, 21129001, 51272006, 51432002, and 51121091).

■ REFERENCES

(1) Waldrop, M. M. *Nature* **2016**, *530*, 144.
(2) Shulaker, M. M.; Hills, G.; Patil, N.; Wei, H.; Chen, H.-Y.; Wong, H. S. P.; Mitra, S. *Nature* **2013**, *501*, 526.
(3) Franklin, A. D. *Nature* **2013**, *498*, 443.
(4) Chen, Y. B.; Zhang, Y. Y.; Hu, Y.; Kang, L. X.; Zhang, S. C.; Xie, H. H.; Liu, D.; Zhao, Q. C.; Li, Q. W.; Zhang, J. *Adv. Mater.* **2014**, *26*, 5898.
(5) Chen, Y. B.; Zhang, J. *Acc. Chem. Res.* **2014**, *47*, 2273.
(6) Hong, S. W.; Banks, T.; Rogers, J. A. *Adv. Mater.* **2010**, *22*, 1826.
(7) Zhou, W. W.; Ding, L.; Yang, S.; Liu, J. *ACS Nano* **2011**, *5*, 3849.
(8) Wu, B.; Geng, D. C.; Guo, Y. L.; Huang, L. P.; Chen, J. Y.; Xue, Y. Z.; Yu, G.; Liu, Y. Q.; Kajiura, H.; Li, Y. M. *Nano Res.* **2011**, *4*, 931.
(9) Hu, Y.; Kang, L. X.; Zhao, Q. C.; Zhong, H.; Zhang, S. C.; Yang, L. W.; Wang, Z. Q.; Lin, J. J.; Li, Q. W.; Zhang, Z. Y.; Peng, L. M.; Liu, Z. F.; Zhang, J. *Nat. Commun.* **2015**, *6*, 6099.
(10) Kang, L.; Hu, Y.; Zhong, H.; Si, J.; Zhang, S.; Zhao, Q.; Lin, J.; Li, Q.; Zhang, Z.; Peng, L.; Zhang, J. *Nano Res.* **2015**, *8*, 3694.
(11) Li, J. H.; Liu, K. H.; Liang, S. B.; Zhou, W. W.; Pierce, M.; Wang, F.; Peng, L. M.; Liu, J. *ACS Nano* **2013**, *8*, 554.
(12) Ding, L.; Tselev, A.; Wang, J. J.; Yuan, D. N.; Chu, H. B.; McNicholas, T. P.; Li, Y.; Liu, J. *Nano Lett.* **2009**, *9*, 800.
(13) Che, Y.; Wang, C.; Liu, J.; Liu, B.; Lin, X.; Parker, J.; Beasley, C.; Wong, H. S. P.; Zhou, C. *ACS Nano* **2012**, *6*, 7454.
(14) Li, W.-S.; Hou, P.-X.; Liu, C.; Sun, D.-M.; Yuan, J.; Zhao, S.-Y.; Yin, L.-C.; Cong, H.; Cheng, H.-M. *ACS Nano* **2013**, *7*, 6831.
(15) Jourdain, V.; Bichara, C. *Carbon* **2013**, *58*, 2.
(16) Khalilov, U.; Bogaerts, A.; Neyts, E. C. *Nat. Commun.* **2015**, *6*, 10306.
(17) Rao, F.-B.; Li, T.; Wang, Y.-L. *Phys. E* **2008**, *40*, 779.
(18) Couttenye, R. A.; De Vila, M. H.; Suib, S. L. *J. Catal.* **2005**, *233*, 317.
(19) Zhang, G.; Qi, P.; Wang, X.; Lu, Y.; Li, X.; Tu, R.; Bangsaruntip, S.; Mann, D.; Zhang, L.; Dai, H. *Science* **2006**, *314*, 974.
(20) Zhang, G.; Qi, P.; Wang, X.; Lu, Y.; Mann, D.; Li, X.; Dai, H. *J. Am. Chem. Soc.* **2006**, *128*, 6026.
(21) Dresselhaus, M. S.; Dresselhaus, G.; Saito, R.; Jorio, A. *Phys. Rep.* **2005**, *409*, 47.
(22) Bachilo, S. M.; Strano, M. S.; Kittrell, C.; Hauge, R. H.; Smalley, R. E.; Weisman, R. B. *Science* **2002**, *298*, 2361.
(23) Strano, M. S.; Dyke, C. A.; Usrey, M. L.; Barone, P. W.; Allen, M. J.; Shan, H.; Kittrell, C.; Hauge, R. H.; Tour, J. M.; Smalley, R. E. *Science* **2003**, *301*, 1519.
(24) Hasegawa, K.; Noda, S.; Sugime, H.; Kakehi, K.; Maruyama, S.; Yamaguchi, Y. *J. Nanosci. Nanotechnol.* **2008**, *8*, 6123.

DOI: 10.1021/jacs.6b03527
J. Am. Chem. Soc. 2016, 138, 6727−6730